

Analysis of Anticaries Potential of Pit and Fissures Sealants Containing Amorphous Calcium Phosphate Using Synchrotron Microtomography

ACB Delben • M Cannon • AEM Vieira
MD Basso • M Danelon • MRE Santo
SR Stock • X Xiao • F De Carlo

Clinical Relevance

The combination of fluoride and resin sealants containing amorphous calcium phosphate was highly effective at preventing the demineralization of enamel.

SUMMARY

The aim of this study was to analyze the anticaries potential of pit and fissure sealants containing amorphous calcium phosphate

*Alberto C. B. Delbem, DDS, MS, PhD, associate professor, Unesp - Univ Estadual Paulista, Araçatuba School of Dentistry, Department of Public Health and Pediatric Dentistry, Araçatuba, Brazil

Mark, Cannon, PhD, professor, Feinberg School of Medicine, Northwestern University, Ann and Robert Lurie Children's Chicago, IL, USA

Ana E. M. Vieira, PhD, postdoctoral, Unesp - Univ Estadual Paulista, Araçatuba School of Dentistry, Department of Public Health and Pediatric Dentistry, Araçatuba, Brazil

Maria D. Basso, MSc, postgraduate, Unesp - Univ Estadual Paulista, Araçatuba School of Dentistry, Department of Public Health and Pediatric Dentistry, Araçatuba, Brazil

Marcelle Danelon, PhD, postdoctoral, Unesp - Univ Estadual Paulista, Araçatuba School of Dentistry, Department of Public Health and Pediatric Dentistry, Araçatuba, Brazil

(ACP) by synchrotron microtomography. Bovine enamel blocks (4×4 mm; n=50) were selected through surface hardness (Knoop) analysis. Slabs were obtained through cross-

Márcia R. E. Santo, undergraduate student, Unesp - Univ Estadual Paulista, Araçatuba School of Dentistry, Department of Public Health and Pediatric Dentistry, Araçatuba, Brazil

Stuart R. Stock, PhD, professor, Feinberg School of Medicine, Northwestern University, Department of Molecular Pharmacology and Biological Chemistry, Chicago, IL, USA

Xianghui Xiao, PhD, Beamline scientist, Argonne National Laboratory, Lemont, IL, USA

Francesco De Carlo, PhD, Beamline scientist, Argonne National Laboratory, Lemont, IL, USA

*Corresponding author: Rua José Bonifácio, 1193, Araçatuba, São Paulo 16015-050, Brazil; e-mail: adelbem@foa.unesp.br

DOI: 10.2341/13-325-L

sections taken 1 mm from the border of the enamel. Five indentations, spaced 100 μm apart, were made 300 μm from the border. Ten specimens were prepared for each tested material (Ultrasal XT plus TM, Aegis, Embrace, Vitremer and Experimental Sealant). The materials were randomly attached to the sectioned surfaces of the enamel blocks and fixed with sticky wax. The specimens were submitted to pH cycling. After that, the surface hardness (SH_1) was determined, and the blocks were submitted to synchrotron microcomputed tomography analysis to calculate the mineral concentration ($\Delta\text{g}_{\text{HAP}} \text{ cm}^{-3}$) at different areas of the enamel. The comparison between the SH_1 and $\Delta\text{g}_{\text{HAP}} \text{ cm}^{-3}$ showed a correlation for all groups ($r=0.840$; $p<0.001$). The fluoride groups presented positive values of $\Delta\text{g}_{\text{HAP}} \text{ cm}^{-3}$, indicating a mineral gain that was observed mainly in the outer part of the enamel. The ACP showed mineral loss in the outer enamel compared with fluoride groups, although it inhibited the demineralization in the deeper areas of enamel. The combination of two remineralizing agents (fluoride and ACP) was highly effective in preventing demineralization.

INTRODUCTION

Amorphous calcium phosphate (ACP) has been identified as a possible precursor in the formation of hydroxyapatite. Dental applications based on the unique characteristics of ACP have been proposed, and it has been shown that the properties of ACP are enhanced when used with similar products that have anti-demineralizing and remineralizing potential.¹ The systems developed use casein phosphopeptides (CPPs) to stabilize the calcium phosphate ions at high concentrations; these include amorphous nano-complexes designated CPP-ACP on the enamel surface.² Incorporating CPP-ACP into glass-ionomer cements improved the anticariogenic potential of this material without adversely affecting its mechanical properties.^{3,4} Recent studies show that composites containing ACP can release supersaturated levels of calcium and phosphate ions in proportions favorable for apatite formation.⁵⁻⁸ In these composites, the addition of ACP led to failures due to degraded mechanical strength; thus, they are not indicated as restorative or lining materials but can be adequate as pit and fissure sealants.^{5,9}

As a sealant, two studies (*in vitro* and *in situ*) showed that the ACP sealant presented the same

capacity of remineralization as the fluoride sealant.^{7,10} When the sealant product contained ACP and fluoride (ACP-F), there was no improvement in its remineralizing effect.⁷ However, it is important to determine if the ACP sealant has the ability to inhibit enamel demineralization because caries is a dynamic process that involves demineralization and remineralization. If it is determined that sealants with ACP-F act as a favorable alternative process for remineralization of the enamel compared with resin agents that contain only fluoride, practitioners would have an additional method for preventing dental caries. The purpose of this study was to analyze the anticaries potential of an ACP sealant and an ACP-F sealant using a pH-cycling model and synchrotron microtomography.

METHODS AND MATERIALS

Preparation and Selection of Enamel Blocks

Enamel blocks (4 mm×4 mm×3 mm; n=50) were obtained from bovine incisor teeth that were stored in 2% formaldehyde solution with a pH of 7.0 for 30 days.¹¹ The enamel surface of the blocks was then serially polished, and the slabs were cross-sectioned at 1 mm from the border (Figure 1A), resulting in specimens with an area of 12 mm².¹¹ The blocks were subjected to surface hardness (Knoop) analysis (SH) using a microhardness tester (Shimadzu MicroHardness Tester HMV-2000, Shimadzu Corp, Kyoto, Japan) with a Knoop diamond under a 25g load for 10 seconds.¹¹ Five indentations spaced 100 μm from each other were made at a distance of 300 μm from the enamel sectioned border (Figure 1B). Enamel blocks with hardness values between 330 and 370 kgf/mm² were selected.

Sample Preparation and Enamel Block Adaptation

Ten samples were prepared for each tested material (Table 1) using a metallic matrix (4 mm×2 mm×1 mm) (Figure 1C) following the manufacturer's instructions, with the exception of the Vitremer (3M ESPE, St Paul, MN, USA), which had a diluted mix at 1/4 the powder to liquid ratio.^{11,12} Polymerization of the materials was performed with a VIP unit (BISCO, Schaumburg, IL, USA) for 40 seconds on both sides of the specimen, using a light intensity of 500 mW/cm². After the sample preparation (Figure 1D), the materials were randomly attached to the sectioned surfaces of the bovine enamel blocks (Figure 1E) and fixed with sticky wax (Kota Industria and Comércio Ltda, São Paulo, Brazil) (Figure 1F).¹¹ The specimens (enamel block +

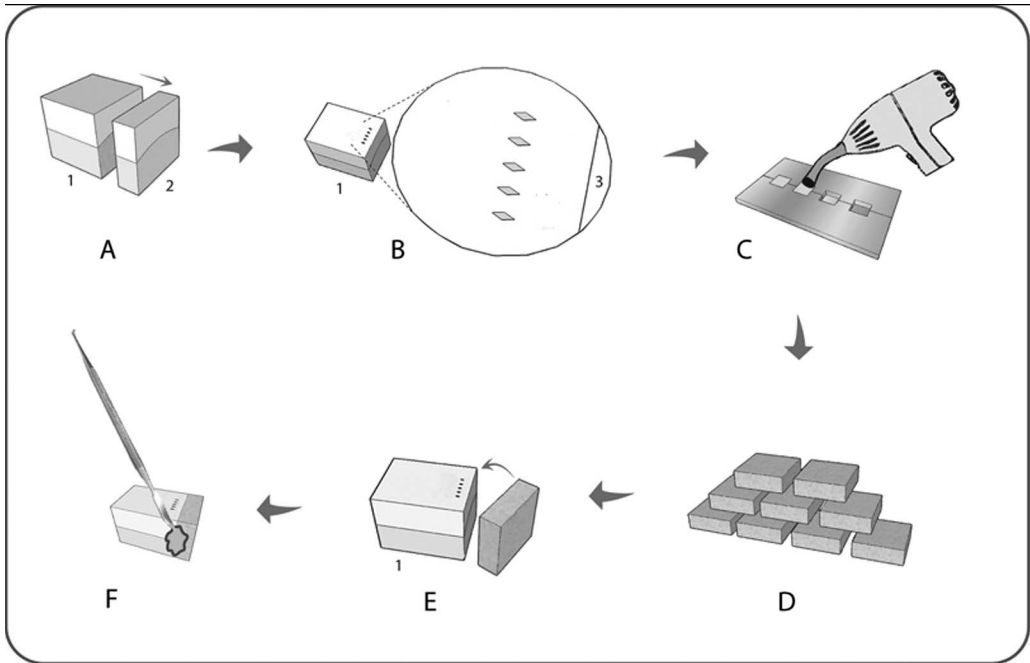


Figure 1. Schematic presentation. (A) Section of the block (1. block 3×4 mm used in the research; 2. Piece of the block 1×4 mm discarded). (B) Five indentations at 300 μm from the enamel sectioned border (3). (C) Polymerization of sample. (D) Samples. (E) Samples adapted onto the enamel blocks (3). (F) Samples fixed with wax.¹¹

sample) were then coated with an acid-resistant varnish, except for the enamel and sample surface.

pH Cycling

The effect of the material in interfering with the dynamic caries process was evaluated. To simulate the demineralization and remineralization process *in vitro*, all specimens were immersed in demineralizing solution for six hours (2.0 mmol/L Ca and P, 0.075 mol/L acetate buffer, 0.04 ppm F, 2.2 mL/mm² of the enamel surface, pH 4.7) and remineralizing solution for 18 hours (1.5 mmol/L Ca, 0.9 mmol/L P, 0.15 mol/L KCl, 0.02 mol/L Tris buffer, 0.05 ppm F, 1.1 mL/mm² of the enamel surface, pH 7.0) for five days at 37°C. The specimens were then submerged in the remineralizing solution for an additional two days before the surface hardness analysis.¹¹

Surface Hardness Analysis

The surface hardness analysis was performed using a Shimadzu HMV-2000 (Shimadzu Corp) microhardness tester and a Knoop diamond under a 25g load for 10 seconds. Five indentations spaced 100 μm from each other were made on the slab surface at 300 μm from the sectioned enamel border (Figure 1B).¹¹ After the pH cycling, the final surface hardness (SH₁) was measured, following the aforementioned methodology.

Analysis of Synchrotron Microcomputed Tomography

Five blocks of each group were sectioned longitudinally and transversely; the samples (1.5 mm×2.0 mm) were then submitted to synchrotron microcomputed tomography at an Advanced Photon

Table 1: Identification of the Tested Material				
Material	Manufacturer	Classification	Batch No.	Group
Ultrasal XT plus	Ultradent Products Inc, South Jordan, UT, USA	Light-cured resin sealant	B 0997	Resin no-F
Aegis	Bosworth Company, Skokie, IL, USA	Light-cured ACP resin sealant	0407-397	Resin ACP
Experimental sealant	Bosworth Company, Skokie, IL, USA	Light-cured ACP and F resin sealant	HJB6-203A	Resin ACP-F
Embrace	Pulpdent Corporation, Watertown, MA, USA	Light-cured F resin sealant	040923	Resin F
Vitremer	3M/ESPE, St Paul, MN, USA	Resin-modified glass ionomer cement	22015	Ionomer
Abbreviations: ACP, amorphous calcium phosphate; F, fluoride.				

Table 2: Analysis of Surface Hardness (SH_1), Integrated Loss of Subsurface Mineral ($\Delta g_{HAP} \text{ cm}^{-3}$), and Integrated Differential Mineral Concentration (ΔIML) According to Groups^a

Groups	SH_1 (kgf/mm ²)	$\Delta g_{HAP} \text{ cm}^{-3}$	$\Delta IML, g_{HAP} \text{ cm}^{-3}$	
			Zone A (2.8–33.6 μm)	Zone B (36.4–89.6 μm)
Resin no-F	47.9 ^a (20.8)	−15.6 ^a (4.5)	−19.8 ^{Aa} (5.5)	−7.9 ^{Aa} (10.2)
Resin F	285.6 ^b (21.3)	0.3 ^b (1.9)	0.7 ^{Ab} (4.0)	0.6 ^{Aa,b} (6.7)
Resin ACP	94.7 ^c (45.1)	−7.3 ^c (1.3)	−3.0 ^{Ab} (4.4)	3.8 ^{Ab} (9.4)
Resin ACP-F	213.9 ^d (37.0)	2.5 ^b (3.7)	1.8 ^{Ab} (4.6)	−1.0 ^{Aa,b} (3.9)
Ionomer	288.9 ^b (19.8)	10.5 ^d (2.3)	5.4 ^{Ab} (3.8)	2.6 ^{Ab} (5.4)

Abbreviations: ACP, amorphous calcium phosphate; F, fluoride.

^a Distinct superscript lowercase letters indicate statistical significance in each analysis (Student-Newman-Keuls test; $p < 0.05$). Distinct superscript capital letters indicate the differences between zones A and B in each line (Student-Newman-Keuls test; $p < 0.05$).

Source 2-BM bending magnet station (Argonne National Laboratory, Argonne, IL, USA). X-ray photons with an energy of 20 keV were provided by a double multilayer monochromator.¹³ The detector system consisted of a 12-bit, CoolSNAP 2K \times 2K CCD camera (Princeton Instrument, New Jersey, USA) coupled with an optical lens (2.5 \times) to a CdWO₄ single-crystal phosphor. Views were recorded every 0.25° from 0° to 180° and were normalized for the detector and beam nonuniformities. Specimens were reconstructed on a 2K \times 2K grid of isotropic voxels, side length \sim 2.8 μm . The analysis was based on mineral concentrations calculated from the linear attenuation coefficient (μ) and described as mass of pure hydroxyapatite ($\rho = 3.15 \text{ g cm}^{-3}$) per unit volume of tissue ($g_{HAP} \text{ cm}^{-3}$).¹⁴

The integrated area under the curve (cross-sectional mineral profiles into the enamel; Figure 1a), using mineral concentration values ($g_{HAP} \text{ cm}^{-3}$) was calculated and the integrated loss of subsurface mineral ($\Delta g_{HAP} \text{ cm}^{-3}$) determined.¹⁵ The differential mineral concentration profiles (Figure 1b) for the materials and mineral concentrations of sound enamel (ie, $g_{HAP} \text{ cm}^{-3}$ value of materials minus $2.40 g_{HAP} \text{ cm}^{-3}$) at each of the material groups were also calculated. These differential profiles were then integrated over two depth zones in the lesion and underlying sound enamel to yield the ΔIML values.¹⁶ Zone boundaries were selected at 33.6 and 89.6 μm to highlight differences in the mineral concentration at different depths.

Statistical Analysis

Analyses were performed using the SigmaPlot software (version 12.0, Systat Software Incorporation, San Jose, CA, USA), and the level of statistical significance was established at 5%. After confirmation of the normal (Shapiro-Wilk) and homogeneous (Cochran) distributions, the data from the SH_1 and

$\Delta g_{HAP} \text{ cm}^{-3}$ were submitted to one-way analysis of variance, followed by the Student-Newman-Keuls test. The results from the ΔIML were submitted to two-way analysis of variance, followed by the Student-Newman-Keuls test. The Pearson's correlation coefficient was calculated for the SH_1 and $\Delta g_{HAP} \text{ cm}^{-3}$.

RESULTS

The surface hardness data of the enamel before the pH cycling exhibited similar mean values (352.1–356.0 kgf/mm²; $p = 0.755$). The resin no-F group showed the lowest values of hardness after the pH-cycling ($p = 0.001$) when compared to the other groups (Table 2). The resin F and ionomer groups showed similar values of hardness ($p = 0.807$) and were higher than the other groups ($p < 0.001$).

The mean of mineral concentration values for sound bovine enamel of the blocks was 2.40 ± 0.06 (2.28–2.54) $g_{HAP} \text{ cm}^{-3}$. The results of the $\Delta g_{HAP} \text{ cm}^{-3}$ (Table 2) showed that treatment with ionomer, resin ACP-F, and resin F did not present with mineral loss. Resin ACP reduced the mineral loss compared with the resin no-F ($p < 0.001$). The combined fluoride/ACP (resin ACP-F group) had an improved resistance against mineral loss, presenting similar values when compared with the resin F group ($p > 0.264$).

The profiles of mineral concentration (Figure 2a) showed a subsurface lesion from the resin no-F and resin ACP. The enamel closer (2.8–5.6 μm) to ionomer ($2.82 \pm 0.25 g_{HAP} \text{ cm}^{-3}$), resin ACP-F ($2.75 \pm 0.20 g_{HAP} \text{ cm}^{-3}$), resin F ($2.61 \pm 0.08 g_{HAP} \text{ cm}^{-3}$) and resin ACP ($2.61 \pm 0.20 g_{HAP} \text{ cm}^{-3}$) presented hypermineralization at 2.8 μm ($p = 0.133$). These groups did not show the formation of a subsurface lesion, except for the resin ACP group. The resins with fluoride and/or ACP presented the same results ($p = 0.156$) at the outer enamel (zone A). However, in

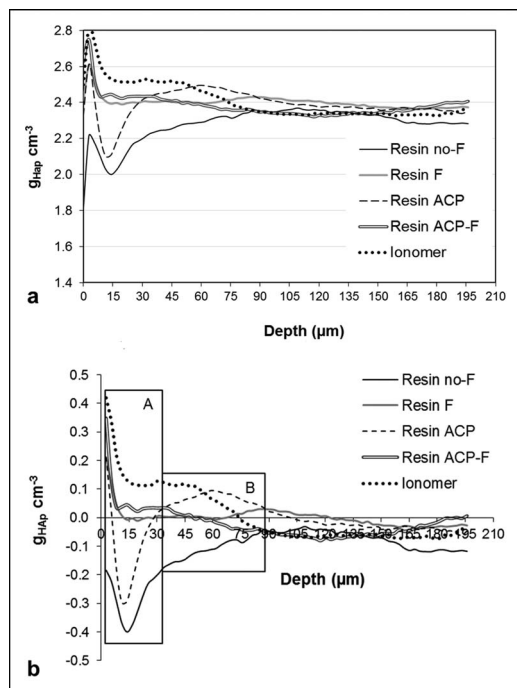


Figure 2. (a) Depth profiles of mineral concentration ($g_{HAP} \text{ cm}^{-3}$) in lesions for each group. (b) Differential mineral concentration profiles ($g_{HAP} \text{ cm}^{-3}$ vs depth) calculated by subtracting resin profiles from sound enamel value ($2.40 g_{HAP} \text{ cm}^{-3}$). Positive values thus indicate a higher mineral concentration at the given depth in the resin groups than the sound enamel, and vice versa. Differential profiles were integrated into each of the marked zones (A–B) to give depth-dependent ΔIML values.

the depth of the lesion (zone B, 36.4–89.6 μm), the resin ACP showed higher mineral concentration ($p=0.038$) along with the ionomer ($p=0.049$) when compared with the resin no-F (Table 2 and Figure 2b).

DISCUSSION

Because ACP is capable of increasing the calcium and phosphate concentrations within a lesion, it has been added to dental products as a remineralizing agent. The addition of ACP in sealant improves the enamel remineralization, as does a fluoride sealant, even presenting different forms of apatite deposition.^{7,10} The capacity of ACP deposits on the enamel surface to inhibit the enamel demineralization has not yet been studied. Besides the *in vitro* demineralization produced in the present study, marginal adaptation failed between the material and enamel, a problem that can occur *in vivo*. The present study showed that ACP released by the sealant led to limited effects against demineralization, but combining it with fluoride can improve its effects. For this study, CPPs were not used to stabilize fluoride and ACP.

The calcium and phosphate release from the resin ACP led to supersaturation of the biofilm with respect to the hydroxyapatite as observed in previous research.⁸ In the present study, these products were able to reduce the mineral loss, thus increasing the mineral concentration on the enamel surface to the same degree as the fluoride materials. This effect is mainly a product of the ionic activity product of the CaHPO_4^0 and the buffering capacity of the ACP.^{8,17} These mineral depositions do not contribute to recovery of the prismatic structure and consequent mechanical properties. The mineral deposition produced by the ACP sealant between 2.8 and 5.6 μm was able to attenuate the X-ray photons but it seems this did not lead to the mechanical restructuring of the prismatic structure as the hardness was lower for this group. Moreover, the supersaturation of the biofilm with respect to the hydroxyapatite produced by resin ACP was not able to reduce the mineral loss in the enamel subsurface at a depth between 8.4 μm and 28.0 μm, where the acid activity should be more intense. However, the ACP can produce a great flux of calcium and phosphate in the deeper part of the enamel,¹⁸ leading to a great mineral gain as observed in the present study in the depth of 36.4 μm to 89.6 μm.

Nevertheless, the fluoride materials are able to increase the biofilm saturation with respect to hydroxyapatite and fluorapatite.⁸ This can explain the higher mineral concentration of the enamel, mainly at the enamel surface. Greater ionic activity does not occur just for the CaHPO_4^0 product but also for the HF^0 .^{8,17} This leads to the effect being mainly on the surface.¹⁸ The mineral deposited in the enamel surface is harder in the presence of fluoride, but there was not a total recovery of the surface hardness. As the ionomer group was prepared with a powder/liquid ratio (¼:1) that leads to higher fluoride release,^{11,12} this can explain the greater anticaries effects.¹¹

Adding fluoride to resin with ACP (ACP-F resin group) improved the capacity to inhibit the demineralization to a similar degree as the fluoride materials. Probably, this is because the resin ACP-F led to an increase in saturation with respect to the hydroxyapatite and fluorapatite. Because the ACP in the resin materials is stabilized by hybridization with ions such as Zr^{2+} or SiO_4^{4-} ,^{5,6} adding sodium fluoride is possible without ACP to react to the fluoride in the composite body. These associations can present a greater ionic activity of the CaHPO_4^0 and HF^0 products which is important mainly in the remineralization of the enamel.^{8,17} This might have

produced a greater effect on the process of remineralization than demineralization, even with increased cariogenic challenge. The data from the mineral concentration profile (Figure 2) support this observation as there was an increase in the $\Delta g_{\text{HAP}} \text{ cm}^{-3}$ values. This can explain the hypermineralization at 30 μm from the enamel surface.

CONCLUSION

The present study showed that the ACP inhibits demineralization in the deeper part of enamel, whereas the fluoride products had a greater effect at the outer part of the enamel. The combination of two remineralizing agents (fluoride and ACP) was highly effective in preventing demineralization.

Conflict of Interest

The authors have no proprietary, financial, or other personal interest of any nature or kind in any product, service, and/or company that is presented in this article.

(Accepted 9 April 2014)

References

1. Regnault WF, Icenogle TB, Antonucci JM, & Skrtic D (2008) Amorphous calcium phosphate/urethane methacrylate resin composites. I. Physicochemical characterization *Journal of Materials Science: Materials in Medicine* **19**(2) 507–515.
2. Cross KJ, Huq NL, Stanton DP, Sum M, & Reynolds EC (2004) NMR studies of a novel calcium, phosphate and fluoride delivery vehicle- α s1casein (59-79) by stabilized amorphous calcium fluoride phosphate nanocomplexes *Biomaterials* **25**(20) 5061–5069.
3. Mazzaoui SA, Burrow MF, Tyas MJ, Daspher SG, Eakins D, & Reynolds EC (2003) Incorporation of casein phosphopeptide-amorphous calcium phosphate into a glass-ionomer cement *Journal of Dental Research* **82**(11) 914–918.
4. Zraikat HA, Palamara JEA, Messer HH, Burrow MF, & Reynolds EC (2011) The incorporation of casein phosphate into a glass ionomer cement *Dental Materials* **27**(3) 235–243.
5. Skrtic D, Hailer AW, Takagi S, Antonucci JM, & Eanes ED (1996) Quantitative assessment of the efficacy of amorphous calcium phosphate/methacrylate composites in remineralizing caries-like lesions artificially produced in bovine enamel *Journal of Dental Research* **75**(9) 1679–1686.
6. Combes C, & Rey C (2010) Amorphous calcium phosphates: Synthesis, properties and uses in biomaterials *Acta Biomaterialia* **6**(9) 3362–3378.
7. Silva KG, Pedrini D, Delbem AC, Ferreira L, & Cannon M (2010) In situ evaluation of the remineralizing capacity of pit and fissure sealants containing amorphous calcium phosphate and/or fluoride *Acta Odontologica Scandinavica* **68**(1) 11–18.
8. Ferreira L, Pedrini D, Okamoto AC, Jardim EG Jr, Henriques TA, Cannon M, & Delbem ACB (2013) Biochemical and microbiological characteristics of in situ biofilm formed on materials containing fluoride or amorphous calcium phosphate *American Journal of Dentistry* **26**(6) 207–213.
9. Skrtic D, Antonucci JM, Eanes ED, & Eidelman N (2004) Dental composites based on hybrid and surface modified amorphous calcium phosphates *Biomaterials* **25**(7–8) 1141–1150.
10. Choudhary P, Tandon S, Ganesh M, & Mehra A (2012) Evaluation of the remineralization potential of amorphous calcium phosphate and fluoride containing pit and fissure sealants using scanning electron microscopy *Indian Journal of Dental Research* **23**(2) 157–163.
11. Rodrigues E, Delbem AC, Pedrini D, & de Oliveira MS (2008) Ph-cycling model to verify the efficacy of fluoride-releasing materials in enamel demineralization *Operative Dentistry* **33**(6) 658–665.
12. Bombonatti JFS, Navarro MFL, Elias ER, Buzalaf MAR, Lauris JRP, & Delbem ACB (2003) Fluoride release of Vitremer in different powder/liquid ratio compared to two pit and fissure sealants *Journal of Medical and Biological Sciences* **2**(2) 201–207.
13. Chu YS, Liu C, Mancini DC, de Carlo F, Macrander AT, & Shu D (2002) Performance of a double multilayer monochromator at 2-BM at the Advanced Photon Source *Review of Scientific Instruments* **73**(3) 1485–1487.
14. Delbem ACB, Sasaki KT, Vieira AEM, Rodrigues E, Bergamaschi M, Stock SR, Cannon ML, Xiao X, De Carlo F, & Delbem ACB (2009) Comparison of methods for evaluating mineral loss: Hardness versus synchrotron microcomputed tomography *Caries Research* **43**(5) 359–365.
15. Delbem AC, Danelon M, Sasaki KT, Vieira AE, Takeshita EM, Brighenti FL, & Rodrigues E (2010) Effect of rinsing with water immediately after neutral gel and foam fluoride topical application on enamel remineralization: An in situ study *Archives Oral Biology* **55**(11) 913–918.
16. Takeshita EM, Exterkate RAM, Delbem ACB, & ten Cate JM (2011) Evaluation of different fluoride concentrations supplemented with trimetaphosphate on enamel de- and remineralization in vitro *Caries Research* **45**(5) 494–497.
17. Cochrane NJ, Saranathan S, Cai F, Cross KJ, & Reynolds EC (2008) Enamel subsurface lesion remineralisation with casein phosphopeptide stabilised solutions of calcium, phosphate and fluoride *Caries Research* **42**(2) 88–97.
18. Langhorst SE, O'Donnell JNR, & Skrtic D. In vitro remineralization of enamel by polymeric amorphous calcium phosphate composite: Quantitative microradiographic study *Dental Materials* **25**(7) 884–891.